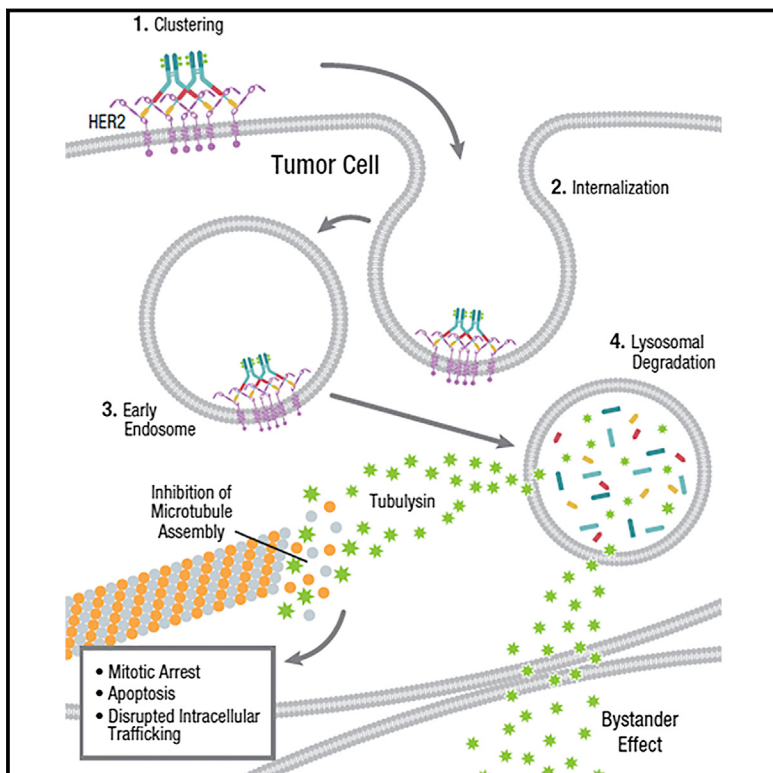


Cancer Cell

A Biparatopic HER2-Targeting Antibody-Drug Conjugate Induces Tumor Regression in Primary Models Refractory to or Ineligible for HER2-Targeted Therapy

Graphical Abstract



Authors

John Y. Li, Samuel R. Perry,
Vanessa Muniz-Medina, ...,
Rakesh Dixit, Jane K. Osbourn,
Steven R. Coats

Correspondence

lij@medimmune.com

In Brief

Li et al. develop a biparatopic HER2-targeting antibody-drug conjugate that demonstrates therapeutic activity in breast cancer models representing T-DM1 eligible, resistant, and ineligible patient populations and has sufficient safety profile in non-human primates to support its translation into clinical trials.

Highlights

- Dual targeting of HER2 by biparatopic ADC enhances toxin delivery into tumor cells
- HER2 biparatopic ADC induces greater breadth of tumor cell killing than T-DM1
- HER2 biparatopic ADC kills tumor cells relapsed/refractory to T-DM1 treatment



A Biparatopic HER2-Targeting Antibody-Drug Conjugate Induces Tumor Regression in Primary Models Refractory to or Ineligible for HER2-Targeted Therapy

John Y. Li,^{1,*} Samuel R. Perry,¹ Vanessa Muniz-Medina,¹ Xinzhang Wang,^{1,6} Leslie K. Wetzel,² Marlon C. Rebelatto,³ Mary Jane Masson Hinrichs,³ Binyam Z. Bezabeh,⁴ Ryan L. Fleming,⁴ Nazzareno Dimasi,⁴ Hui Feng,^{4,7} Dorin Toader,⁴ Andy Q. Yuan,⁴ Lan Xu,⁴ Jia Lin,⁴ Changshou Gao,⁴ Herren Wu,⁴ Rakesh Dixit,³ Jane K. Osbourn,^{1,5} and Steven R. Coats¹

¹Biosuperiors

²Oncology

³Biologics Safety Assessment

⁴Antibody Discovery & Protein Engineering

MedImmune LLC, Gaithersburg, MD 20878, USA

⁵MedImmune Ltd, Granta Park, Cambridge CB21 6GH, UK

⁶Present address: Merck Research Laboratories, Boston, MA 02115, USA

⁷Present address: Topalliance Bioscience Inc., Menlo Park, CA 94025, USA

*Correspondence: lij@medimmune.com

<http://dx.doi.org/10.1016/j.ccel.2015.12.008>

SUMMARY

Antibody-drug conjugate (ADC) which delivers cytotoxic drugs specifically into targeted cells through internalization and lysosomal trafficking has emerged as an effective cancer therapy. We show that a bivalent biparatopic antibody targeting two non-overlapping epitopes on HER2 can induce HER2 receptor clustering, which in turn promotes robust internalization, lysosomal trafficking, and degradation. When conjugated with a tubulysin-based microtubule inhibitor, the biparatopic ADC demonstrates superior anti-tumor activity over ado-trastuzumab emtansine (T-DM1) in tumor models representing various patient subpopulations, including T-DM1 eligible, T-DM1 ineligible, and T-DM1 relapsed/refractory. Our findings indicate that this biparatopic ADC has promising potential as an effective therapy for metastatic breast cancer and a broader patient population may benefit from this unique HER2-targeting ADC.

INTRODUCTION

Human epidermal growth factor receptor 2 (HER2) is a receptor tyrosine kinase that is involved in the regulation of various cellular functions. Aberrant HER2 receptor activation has been implicated as a driving factor in the tumorigenesis and progression of a number of cancers (Yarden and Sliwkowski, 2001; Tagliabue et al., 2010; Roskoski, 2014). In breast cancer, overexpression and/or amplification of the HER2 gene, identified by immunohistochemistry (HercepTest; Dako) and fluorescence in situ hybridization, is observed in 20%–25% of patients and these patients are classified as HER2-positive in the clinic. Excessive expres-

sion of HER2 often leads to constitutive receptor activation and therefore aggressive tumor growth (Slamon et al., 1987). Inhibiting HER2 activity with monoclonal antibodies has proven to be an effective therapy for treating HER2-positive metastatic breast cancer. To date, three HER2-specific monoclonal antibodies have been approved by regulatory agencies; they are trastuzumab, pertuzumab, and ado-trastuzumab emtansine (T-DM1). Although these HER2-targeting therapies have transformed the clinical practice for HER2-positive breast cancer and have resulted in survival benefits, not all patients respond to the therapies. Moreover, the vast majority of patients who initially respond to the treatment will eventually relapse. This is

Significance

Current HER2-targeted therapeutics are ineffective in killing cancer cells expressing relatively low levels of HER2. Therefore, only about 20% of breast cancer patients are eligible for HER2-targeted therapies and the majority of patients who initially respond to treatment eventually relapse due to intratumoral heterogeneity of HER2 expression. We developed a biparatopic HER2-targeting antibody-drug conjugate (ADC) that demonstrated potent anti-tumor activity in cancer cells expressing a broader range of HER2. Safety studies in non-human primates indicate that the therapeutic index of this biparatopic ADC is sufficient to transition into clinical trials. A phase I clinical trial to assess the safety and preliminary efficacy of the biparatopic ADC is underway in patients refractory to or ineligible for current HER2-targeted therapies.

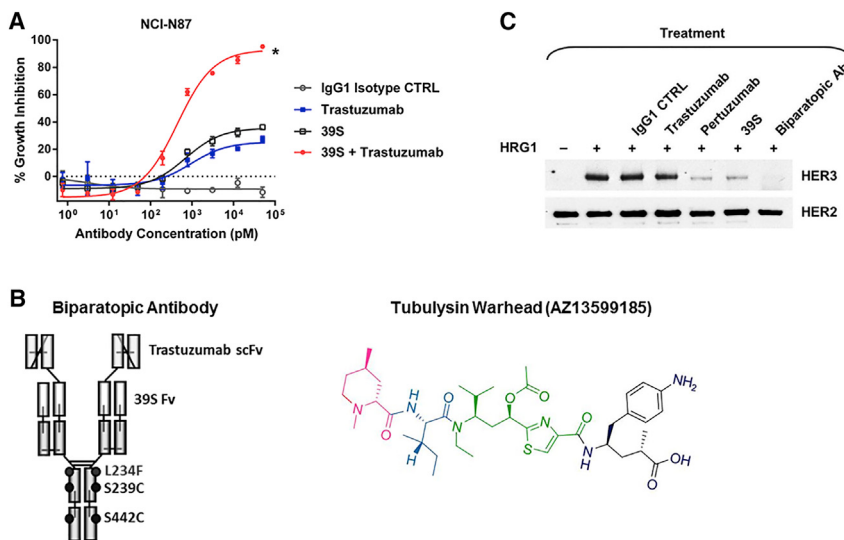


Figure 1. Construction of Anti-HER2 Biparatopic Antibody

(A) The 39S antibody functions synergistically with trastuzumab in inhibiting NCI-N87 cell proliferation in vitro. Representative graph shows the mean percent growth inhibition \pm SEM ($n = 3$). * $p < 0.05$ at all treatment concentrations (at 0.01 type I error level) indicating a strong synergistic effect. See also Figure S1A.

(B) Schematic of the HER2-specific biparatopic antibody and the tubulysin variant AZ13599185.

(C) The biparatopic antibody blocks ligand-induced HER2-HER3 receptor dimerization in T47D cells. Serum-starved T47D cells were incubated for 10 min in the presence (+) or absence (-) of heregulin-1 β (HRG1, 1 nM) and antibody (5 nM in concentration for each antibody) and then lysed. Cell lysates were immunoprecipitated with an HER2-specific antibody and the HER2-HER3 immunocomplex was detected by western blot. Immunoblots show the formation of HER2-HER3 complex in response to the treatment.

thought to be due to the high degree of intratumoral heterogeneity of HER2 expression in breast cancer and lack of efficacy of current anti-HER2 therapeutics in tumor cells expressing relatively low levels of HER2. Clinically, these low HER2-expressing tumors are classified as HER2-negative despite that they mostly express HER2 at a higher level than normal tissues. A great deal of effort has been put into developing better anti-HER2 agents that can kill cancer cell populations expressing a broad range of HER2 (Kurata et al., 2014; Nordstrom et al., 2011). Given the lack of clinical success in developing therapies to treat tumors with relatively low levels of HER2, this remains an area of high unmet medical need.

Antibody-drug conjugates (ADCs) are a class of drugs that use antibodies specifically targeting tumor-associated antigens as vehicles to deliver covalently attached small-molecule toxins into cancer cells (Sievers and Senter, 2013). T-DM1 is built upon this principle and it consists of trastuzumab coupled with the microtubule poison maytansinoid DM1 through a thioether linker (Lambert and Chari, 2014; Lewis Phillips et al., 2008). Approval of T-DM1 by the U.S. Food and Drug Administration in February 2013 is mainly based on the key data derived from a phase III clinical trial investigating the efficacy and safety of T-DM1 in HER2-positive metastatic breast cancer patients (Verma et al., 2012). T-DM1 treatment prolonged overall survival by 5–6 months with an objective response rate of 44%. While these results are encouraging, they also reveal the limitation of T-DM1 in efficacy. Receptor tyrosine kinases are typically routed to lysosomes for degradation following ligand binding, which is a major negative feedback mechanism regulating the intensity and duration of receptor activation (Wiley, 2003). Unlike most receptor tyrosine kinases, HER2 has no natural ligand and it appears to be impaired in lysosomal trafficking (Austin et al., 2004; Sorkin and Goh, 2008; Roepstorff et al., 2008). Instead, HER2 is largely recycled back to the plasma membrane following spontaneous endocytosis. Correspondingly, the majority of internalized T-DM1 passively recycles with HER2 back to the cell surface and only a small fraction of T-DM1 is routed to lysosomes for degradation (Austin et al., 2004). Since the amount of toxin released

into the cytoplasm determines the cell killing potency of an ADC, this may explain the lack of activity with T-DM1 in tumors expressing low levels of HER2. In this regard, it is likely that an improvement in ADC-mediated internalization and lysosomal trafficking would significantly enhance the cytoplasmic delivery of toxins, which may result in the killing of cancer cell populations that express a broader range of HER2. In this study, we constructed a biparatopic HER2-targeting ADC, characterized its anti-tumor activity, and evaluated its safety profile and therapeutic potential in treating breast cancer patients who are refractory to or ineligible for current HER2-targeted therapies.

RESULTS

Construction of Anti-HER2 Biparatopic Antibody

Monoclonal antibody 39S is a fully human antibody against HER2. It was derived from a XenoMouse hybridoma clone 1.39.1 that is capable of blocking HER2/HER3 receptor phosphorylation in heregulin-1 β -treated cancer cells (Cartilage et al., 2010). Further characterization of the antibody revealed that it could function synergistically with trastuzumab to inhibit cancer cell proliferation (Figure 1A). This synergistic inhibition effect was confirmed in several relevant in vivo xenograft tumor models (Figure S1A and data not shown). In a cell-based binding competition assay, 39S antibody demonstrated concurrent binding to HER2-expressing cancer cells with trastuzumab and pertuzumab, suggesting that it interacted with a unique epitope on HER2 that was different from these therapeutic antibodies (Figure S1B). By using the variable domain sequences of 39S and trastuzumab, we constructed a biparatopic antibody containing the single-chain variable fragment (scFv) of trastuzumab attached to the N terminus of the heavy chain of 39S IgG₁ (Figure 1B). The resulting antibody construct contains four antigen-binding units, or two on each arm that are capable of interacting with two different epitopes on HER2. Antigen-binding activity determined by ELISA confirmed that this biparatopic antibody retained the HER2 binding specificity of its parental antibodies (Figure S1C). Furthermore, to determine whether

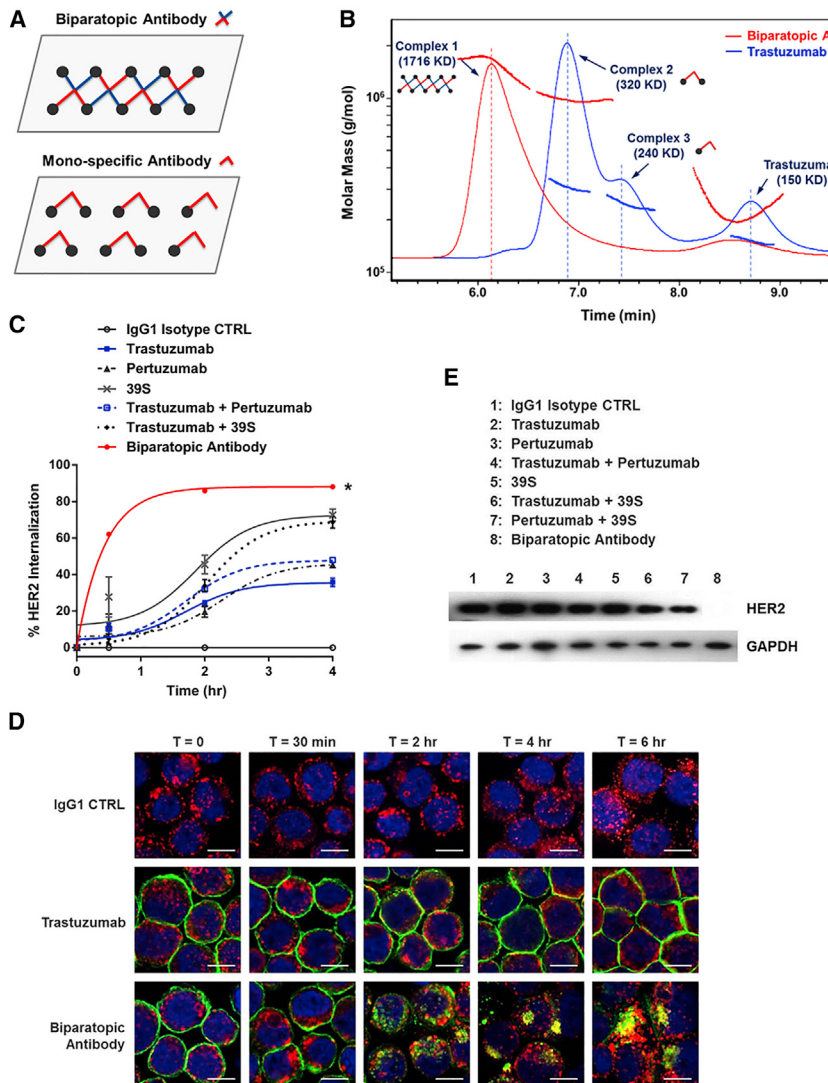


Figure 2. The Biparatopic Antibody Promotes HER2 Clustering and Lysosomal Degradation

(A) Schematics of receptor cross-linking induced by antibody interaction and hypothetical difference in mode of cross-linking between monospecific antibody and biparatopic antibody that targets two non-overlapping epitopes on the receptor. Solid circle (●) represents the receptor. Putative molecular masses for the three immunocomplexes as shown are ~235 kDa, ~320 kDa, and ~1730 kDa. (B) Analysis of immunocomplexes by HPLC SEC-MALS assay. Representative graph shows the relative quantity and size of the HER2-antibody complex formed at a molar ratio of 1:1. See also Figure S2A for results at other molar ratios.

(C) HER2 receptor internalization induced by the biparatopic antibody in comparison with the monospecific antibodies and antibody combinations. Representative graph shows the mean percent internalization \pm SEM ($n = 3$) in BT474 cells. * $p < 0.001$ by Student's *t* test compared with trastuzumab. See also Figure S2B.

(D) Confocal microscopy images of BT474 cells showing HER2 internalization and lysosomal trafficking induced by the biparatopic antibody or trastuzumab (50 nM concentration for each antibody). HER2-antibody complexes were stained by AF488-labeled antibody (green), lysosomes were stained by AF647-labeled antibody (red), and nuclei were stained by DAPI (blue). Scale bars, 5 μ m.

(E) Representative immunoblots of lysates from antibody (500 nM)-treated BT474 cells showing that the biparatopic antibody induces HER2 degradation.

the biparatopic antibody can inhibit ligand-induced HER2-HER3 receptor dimerization, we treated the T47D cells with heregulin-1 β in the presence or absence of antibody and examined the HER2-HER3 interaction by immunoprecipitation and western blot. Results showed that the biparatopic antibody completely blocked HER2-HER3 receptor dimerization induced by heregulin-1 β (Figure 1C). It has been reported that trastuzumab can inhibit the ligand-independent HER2 receptor dimerization (Junttila et al., 2009). This biparatopic antibody contains both the trastuzumab scFv and the 39S Fv units; therefore it is able to block both ligand-independent and ligand-dependent receptor activation, resulting in more effective inhibition of cancer cell proliferation driven by the HER2-mediated signaling pathways.

Biparatopic Antibody Promotes HER2 Clustering and Lysosomal Trafficking

Theoretically, the biparatopic antibody can cross-link HER2 to form a large meshwork structure as shown in Figure 2A, due to its tetravalent binding capacity targeting two non-overlapping epitopes. To test this hypothesis, we mixed the biparatopic anti-

body or trastuzumab with the recombinant human HER2 extracellular domain protein (~85 kDa in mass) at various molar ratios and examined the immunocomplex formation by high-performance liquid chromatography (HPLC) size-exclusion chromatography and multi-angle light scattering (SEC-MALS) assay. Figure 2B shows representative data derived from an antibody/HER2 molar ratio of 1:1 (data with other ratios are shown in Figure S2A). The biparatopic antibody cross-linked multiple HER2 molecules to form a complex as large as 1716 kDa in mass. In contrast, trastuzumab only bound to one or two HER2 molecules to form a 240-kDa or 320-kDa complex, respectively.

It has been reported that receptor clustering at the cell surface can result in rapid receptor internalization, inhibition of recycling, and lysosomal degradation (Friedman et al., 2005; Spangler et al., 2010, 2012). To examine whether the biparatopic antibody can induce enhanced HER2 internalization, we treated BT474 cells with various antibodies and then measured the cell surface level of HER2 by flow cytometry. As shown in Figure 2C, the biparatopic antibody elicited a much faster and higher level of receptor internalization than any monospecific antibody or antibody combination. Similar experiments were conducted in other cell lines with lower levels of HER2 expression; results demonstrated that the extent of enhancement in internalization

Table 1. In Vitro Potency of Anti-HER2 ADC in a Panel of Cancer Cell Lines

Cell Line	Cancer Type	HercepTest	Relative HER2 Density on Cell	In Vitro Cytotoxicity (EC_{50} in pM)	
			(Mean, n = 3)	T-DM1	Biparatopic ADC
SKBR-3	breast	3+	1,517,135	82.6	4.0
NCI-N87	gastric	3+	1,292,978	275.1	23.7
SKOV-3	ovarian	3+	349,178	116.1	8.7
MDA-MB-361	breast	3+/2+	252,249	266.0	4.0
JIMT-1	breast	2+	65,573	inactive	5.1
MDA-MB-453	breast	2+	77,314	344.3	10.5
RT-112	bladder	2+	7,664	inactive	36.5
MCF7-GTU	breast	2+	6,058	inactive	84.5
ZR-75-1	breast	1+	5,892	inactive	18.1
T47D	breast	1+	6,124	inactive	inactive
MCF-7	breast	0	3,646	inactive	inactive
MDA-MB-468	breast	0	undetectable	inactive	inactive

EC_{50} values were determined using Sigmoidal non-linear regression analysis with GraphPad Prism software.

induced by the biparatopic antibody was largely influenced by the HER2 level on the cell surface and it became less significant as the HER2 receptor density decreased (Figure S2B and Table 1). To further illustrate the intracellular trafficking events, confocal microscopy was used to visualize the receptor-antibody internalization and lysosomal trafficking. Representative confocal microscopy images are shown in Figure 2D. Results demonstrated that the biparatopic antibody induced a rapid and robust HER2 receptor internalization and that the internalized immunocomplexes were co-localized with lysosomes. In contrast, trastuzumab only induced a limited HER2 receptor internalization and few complexes were co-localized with lysosomes.

We next asked whether the antibody-HER2 complexes were degraded in the lysosomes following internalization and lysosomal trafficking. To address this question, the total amount of HER2 protein was analyzed from lysates of BT474 cells treated with the antibodies. As shown in Figure 2E, the biparatopic antibody induced HER2 degradation as demonstrated by a lack of HER2 protein in the cell lysate. In contrast, treatment with other anti-HER2 antibodies or antibody combinations showed no significant HER2 degradation.

Biparatopic ADC Demonstrates Potent, Target-Mediated Cytotoxic Activity

Since the biparatopic antibody promotes receptor internalization and lysosomal degradation, it should serve as an effective vehicle to deliver toxins into the target cells in the form of ADC. AZ13599185 is a tubulysin variant developed by AstraZeneca/MedImmune (Figure 1B). The mode of action of this small-molecule toxin is to inhibit microtubule polymerization during mitosis to induce cell death. The biparatopic antibody contains three site mutations in the Fc region, L234F, S239C, and S442C (Figure 1B). The two engineered cysteine residues per heavy chain (S239C and S442C) enable site-specific conjugation of AZ13599185 to the antibody via a maleimidocaproyl linker, resulting in a biparatopic ADC with a drug to antibody ratio of 4. The mutation L234F in combination with the S239C mutation reduced Fc gamma receptor (Fc γ R) binding as determined

by Biacore analysis (data not shown). It is thought that these mutations may minimize the Fc γ R-mediated, HER2-independent uptake of ADC by normal tissues, thereby reducing off-target toxicity such as thrombocytopenia (Uppal et al., 2015). To confirm that the conjugation of tubulysin did not alter the binding characteristics of the biparatopic antibody, we compared binding activities of the biparatopic ADC to its parental unconjugated antibody using ELISA and the Biacore assay. The biparatopic ADC retained the target binding specificity and affinity to HER2 identical to its parental unconjugated antibody (Figure S1C and data not shown).

To evaluate the cytotoxic activity of the biparatopic ADC, a panel of human cancer cell lines expressing different levels of HER2 was selected and their HER2 expression was verified by HercepTest and quantitative flow cytometry (Table 1). For the in vitro cytotoxicity assay, we treated the cells with the biparatopic ADC or T-DM1 and then examined cell viability. The results demonstrated that the cell killing activity was generally correlated to the level of HER2 expression on the cell surface (Figure 3A and Table 1). In HER2 overexpressing cancer cell lines (SKBR-3, NCI-N87, and SKOV-3), both the biparatopic ADC and T-DM1 demonstrated activity, however the biparatopic ADC was at least 10-fold more potent than T-DM1. Furthermore, the biparatopic ADC was active in cancer cells that were intrinsically resistant to T-DM1, represented by JIMT-1, a breast cancer cell line that overexpresses HER2 but is unresponsive to T-DM1 treatment. In cancer cell lines expressing relatively low levels of HER2 (RT-112, MCF7-GTU, and ZR-75-1), the biparatopic ADC also demonstrated potent cell killing activity with median effective concentration (EC_{50}) values <100 pM, whereas T-DM1 was inactive. In cancer cell lines expressing limited levels of HER2 (MDA-MB-468, MCF-7, and T47D), the biparatopic ADC did not induce significant cell death. These in vitro data suggested that the cytotoxic killing by the biparatopic ADC was HER2-dependent and a minimal level of HER2 on the cell surface was required to mediate the intracellular delivery of toxins to induce cell death. To further confirm this observation *in vivo*, we conducted a tumor growth inhibition study with the NCI-H69 xenograft model. NCI-H69 is a small-cell lung cancer model with a

marginally detectable level of HER2 expression by western blot. Weekly dosing of the biparatopic ADC at 3 mg/kg showed no tumor growth inhibition in this model compared with the vehicle control, whereas treatment with the positive control, cisplatin, induced tumor stasis (Figure 3B).

To illustrate the mode of action of the biparatopic ADC, we examined the disruption of the intracellular microtubule network in response to treatment. As shown in Figure 3C, the biparatopic ADC, similar to T-DM1, disrupted the intracellular microtubule network in HER2-overexpressing cells. Experiments performed in multiple cell lines that have different sensitivities to the biparatopic ADC and T-DM1 showed a close correlation between microtubule disruption and in vitro cell killing (Figures S3 and 3A).

Biparatopic ADC Is More Potent than T-DM1 in Tumor Models Representing T-DM1-Eligible Patients

To determine the in vivo anti-tumor activity of the biparatopic ADC, we have tested the molecule in tumor models representing different breast cancer patient subpopulations classified by HER2 expression. ST225 is a primary tumor xenograft model derived from an HER2-positive metastatic breast cancer patient eligible for HER2-targeted therapies. Weekly intravenous administration of the biparatopic ADC, for a total of four doses, led to complete tumor regression and all treated animals remained tumor free for over 120 days after the treatment. In contrast, T-DM1 treatment induced tumor stasis and the tumors regrew soon after the treatment was stopped (Figure 4A). In addition, dosing with a mixture of unconjugated biparatopic antibody and tubulysin at a 1:4 molar ratio (ADMix) or isotype control ADC had no impact on tumor growth, suggesting that the anti-tumor effect of the biparatopic ADC was target mediated. There were no signs of adverse events or weight loss in any of the treatment groups.

The objective response rate of T-DM1 in the clinic is reported to be around 44% (Verma et al., 2012), i.e., over 50% of eligible patients have inherent resistance to T-DM1. To investigate the potential use of the biparatopic ADC in treating T-DM1 unresponsive patients, we tested it in a JIMT-1 xenograft model, which is intrinsically resistant to T-DM1. JIMT-1 cells were injected orthotopically into the mammary fat pads of immune-deficient mice and the tumors were verified for HER2 expression by HercepTest showing 3+. Treatment with T-DM1 or the combination of T-DM1 and pertuzumab showed no significant inhibition of tumor growth. However, the biparatopic ADC induced complete tumor regression and the animals remained tumor free for up to 50 days following the treatment (Figure 4B). These data demonstrate that the biparatopic ADC is more potent than T-DM1 and may provide a therapeutic opportunity for HER2-positive patients with inherent resistance to T-DM1 therapy.

Biparatopic ADC Is Active in Tumor Models with Acquired Resistance to T-DM1

We next sought to examine whether the biparatopic ADC is capable of killing tumor cells that are relapsed/refractory from T-DM1 treatment. To establish the cell lines with acquired resistance to T-DM1, four HER2-overexpressing cancer cell lines that are sensitive to T-DM1 (BT474 [breast], NCI-N87 [gastric], SKOV-3 [ovarian], and MDA-MB-361 [breast]) were treated

with T-DM1 at gradually increasing concentrations in the culture medium. After 4–12 months of continuous treatment, stable resistant cell lines emerged and these cell lines were refractory to at least 1 µg/ml T-DM1 in vitro. Cytotoxic activity of the biparatopic ADC in the T-DM1-resistant cell lines was evaluated by cell killing assays. Results indicated that the biparatopic ADC was capable of inducing substantial growth inhibition in all four T-DM1-resistant cell lines with EC₅₀ < 100 pM (Figure S4). To establish an in vivo tumor model with acquired T-DM1 resistance, we injected the T-DM1-resistant NCI-N87 cells subcutaneously into the immune-deficient mice, and treated the tumor-bearing mice with 3 mg/kg T-DM1. It appeared that the in vitro T-DM1 resistance was not fully translated into the in vivo resistance, reflected by considerable variations in tumor growth among animals. Thus, mice with large refractory tumors (~1,000 mm³ in volume) were selected and the tumor tissue fragments were passaged to new mice until the tumors grew consistently in the presence of weekly treatment of 3 mg/kg T-DM1. After three passages, stable resistant tumors evolved and these tumors were fragmented and implanted into mice to evaluate the in vivo activity of the biparatopic ADC. As demonstrated in Figure 4C, tumors relapsed from the repeated T-DM1 treatment were not only resistant to T-DM1, but also unresponsive to T-DM1 and pertuzumab combination treatment. In contrast, the biparatopic ADC induced a robust and sustained tumor regression after four doses of treatment, showing promise as an effective therapy for the T-DM1 relapsed/refractory patients.

Biparatopic ADC Is Active in Tumor Models Representing T-DM1 Ineligible Patients

The majority of breast cancer patients do not have HER2 gene amplification and/or overexpression in their tumors. Clinically these patients are classified as HER2-negative and are ineligible for the currently approved HER2-targeted therapies. Moreover, a subtype of breast cancer characterized as triple-negative (negative in diagnostic tests for estrogen receptor [ER], progesterone receptor [PR] and HER2) is known to be more aggressive and refractory to many existing therapies (Llombart-Cussac et al., 2014). In particular, triple-negative breast cancer patients have a significant need for new therapies. The unique design of the biparatopic ADC enables it to deliver more toxin into the targeted cancer cells and has shown potent in vitro cytotoxic activities in tumor cells expressing low levels of HER2 (Figure 3A). To determine if this activity translates in vivo, we evaluated the biparatopic ADC in a primary tumor xenograft model derived from a triple-negative breast cancer patient. As shown in Figure 4D, the biparatopic ADC induced complete tumor regression following the treatment, whereas T-DM1 or the control antibody did not inhibit tumor progression. To further expand this finding, we have examined the biparatopic ADC in an additional 16 primary tumor models derived from HER2-negative breast cancer patients. Other criteria were also considered in the selection of these models, including the degree of heterogeneity in HER2 expression, ER/PR status and histopathologic subclass, to maximize the diversity of tumor subtypes in the study. The biparatopic ADC demonstrated potent anti-tumor activity regardless of the histopathologic subclass and ER/PR status of the tumor (Figure 5 and Table 2). In summary, at a dose of 1 mg/kg, 41% of the tumor models showed tumor regression and 6% showed

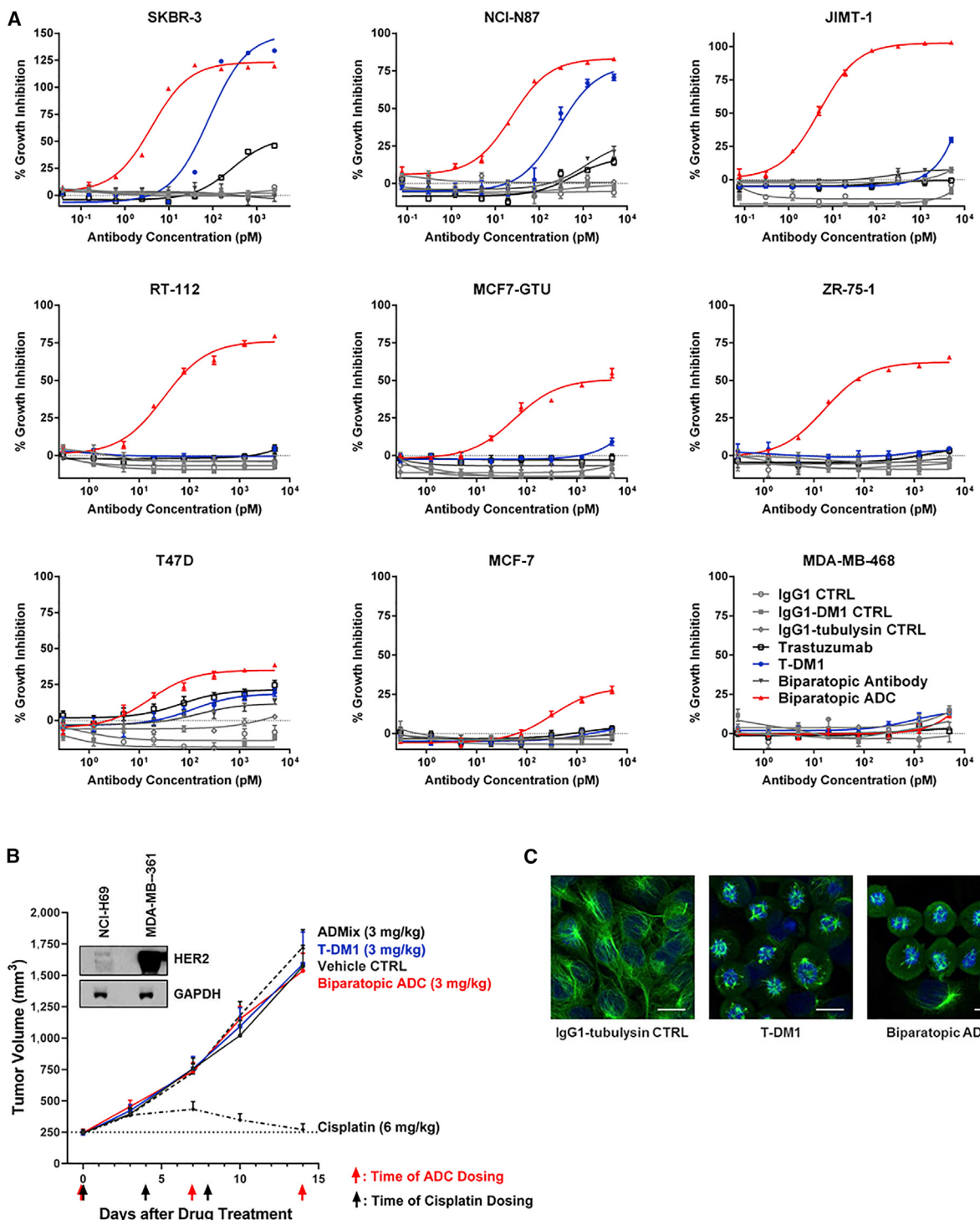


Figure 3. Biparatopic ADC Demonstrates Potent, Target-Mediated Cytotoxic Activity in a Panel of Cancer Cell Lines Expressing Different Levels of HER2

(A) Graphs are representative data derived from different cell lines showing the mean percent growth inhibition \pm SEM ($n = 3$). Quantification of HER2 expression and in vitro potency in EC₅₀ are described in Table 1.

(B) The biparatopic ADC is inactive in the NCI-H69 xenograft model, which expresses a marginally detectable level of HER2 in the tumor. HER2 expression level in the NCI-H69 tumor, relative to the MDA-MB-361 tumor, was verified by western blot analysis. Mice bearing NCI-H69 tumors were dosed weekly with the

(legend continued on next page)

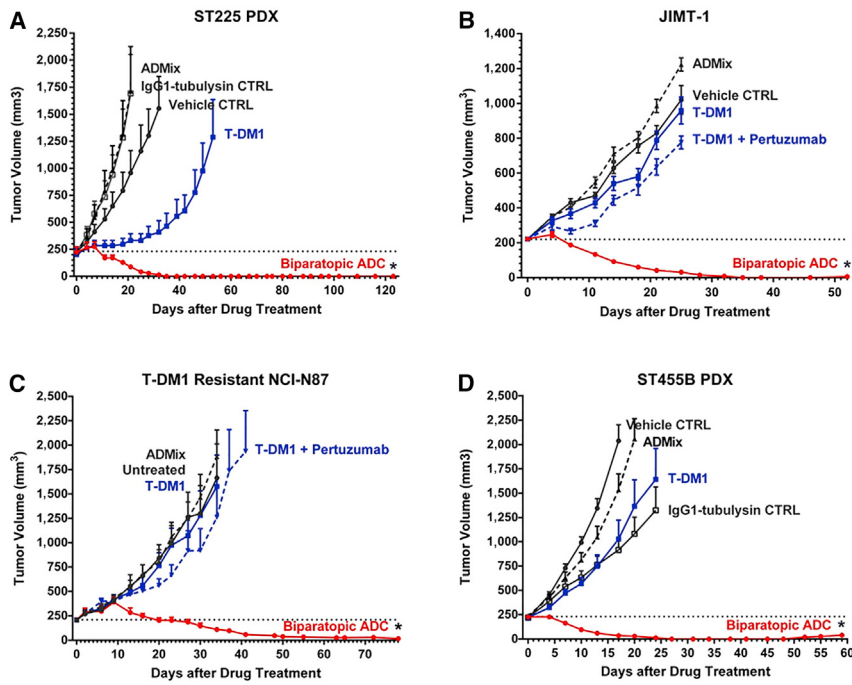


Figure 4. Biparatopic ADC Induces Tumor Regression in In Vivo Xenograft Models Representing Different Patient Subpopulations of Breast Cancer

(A) Primary breast tumor model ST225 represents the HER2-positive/T-DM1 eligible patients.
 (B) JIMT-1 cell line-based tumor model represents the HER2-positive/T-DM1 non-responder patients.
 (C) T-DM1 resistant NCI-N87 tumor model represents the HER2-positive patients relapsed/refractory from the T-DM1 treatment.

(D) Primary breast tumor model ST455B represents the HER2-negative/T-DM1 ineligible patients. Tumor growth curves, in response to weekly intravenous dosing of the biparatopic ADC (3 mg/kg), T-DM1 (3 mg/kg), or other control antibody/ADC (3 mg/kg, except for pertuzumab which is 10 mg/kg) for a total of four doses, showing the mean tumor volume (mm³) ± SEM. ST225, n = 8 or 9; JIMT-1, n = 10; T-DM1 resistant NCI-N87, n = 7; ST455B, n = 10.

*p < 0.001 by Student's t test compared with the untreated or vehicle control group.

tumor stasis. At a dose of 3 mg/kg, 71% of the models showed tumor regression and 12% showed tumor stasis. These results underscore the potential use of the biparatopic ADC to treat a large patient population ineligible for current HER2-targeted therapies.

We have noticed the lack of correlation between the HercepTest score and the in vivo activity of the biparatopic ADC in these 17 patient-derived xenograft (PDX) models (Table 2). The HercepTest is a diagnostic assay for identifying HER2-overexpressing (HER2-positive) patients; it is not optimized for reliable detection of HER2 in the non-overexpressed range. We have attempted to use other commercially available assays, such as the HERmark assay (Monogram Biosciences), to measure the HER2 level in tumors (Huang et al., 2010). Data suggest that the HERmark assay is a more sensitive method, as it can detect a significant amount of HER2 in tumor tissues that have a score of zero by HercepTest (Table 2). This also confirms that the HercepTest is inadequate in differentiating HER2 levels in the non-overexpressed range. The HER2Low Test, which is a highly sensitive immunohistochemistry (IHC) assay using a high-affinity HER2-specific antibody, was recently developed by AstraZeneca and Dako. In an analytical sensitivity study with breast cancer cell lines, the HER2Low Test demonstrated higher reproducibility and repeatability in differentiating lower levels of HER2 compared with the HercepTest (Pedersen et al., 2013). The results of the HER2Low Test are categorized as high (H), medium (M), and low (L). As shown in Table 2, some of the PDX models with undetectable HER2 by HercepTest are actually expressing relatively high levels of HER2, showing high (H) or

less responsive to the biparatopic ADC treatment. Further validation of the HER2Low Test in phase I clinical trials is underway to verify whether it can be used as a companion diagnosis to supplement existing HER2 testing methods for the stratification of patients who would most likely benefit from biparatopic ADC therapy.

Biparatopic ADC Demonstrates Bystander Killing Activity

Immunohistochemistry (IHC) analysis of the 17 PDX models revealed a high heterogeneity of HER2 expression in these tumors. The percent of HercepTest-positive cells varied from undetectable to 70% among the models. Despite such diverse heterogeneity of HER2 expression, treatment with the biparatopic ADC led to sustained tumor regression in many of the models (Table 2). It is hypothesized that the biparatopic ADC may be able to kill non-HER2 expressing tumor cells through a bystander mechanism. Bystander killing by an ADC is mediated by the free cytotoxin that passively diffuses from target-positive cancer cells into the tumor microenvironment, killing neighboring cancer cells that are insensitive to the ADC because of no or limited target expression. A bystander effect is a desired feature for HER2-targeting ADC in the treatment of breast cancer because HER2 expression is frequently heterogeneous in breast tumor tissues (Kovtun and Goldmacher, 2007). A co-culture cell killing assay was performed to determine whether the biparatopic ADC induced a bystander effect. Two cell lines were generated using a lentiviral vector

biparatopic ADC (3 mg/kg), T-DM1 (3 mg/kg), ADMix (3 mg/kg), or vehicle control, or treated with the positive control cisplatin (6 mg/kg) twice a week. Tumor growth curves showing the mean tumor volume (mm³) ± SEM (n = 9).

(C) Confocal microscopy images of SKOV-3 cells showing the mode of action of the biparatopic ADC. Similar to T-DM1, the biparatopic ADC disrupts the intracellular microtubule network following overnight treatment (5 nM each ADC). Microtubules are shown in green and nuclei shown in blue. Scale bars, 10 μm. See also Figure S3.

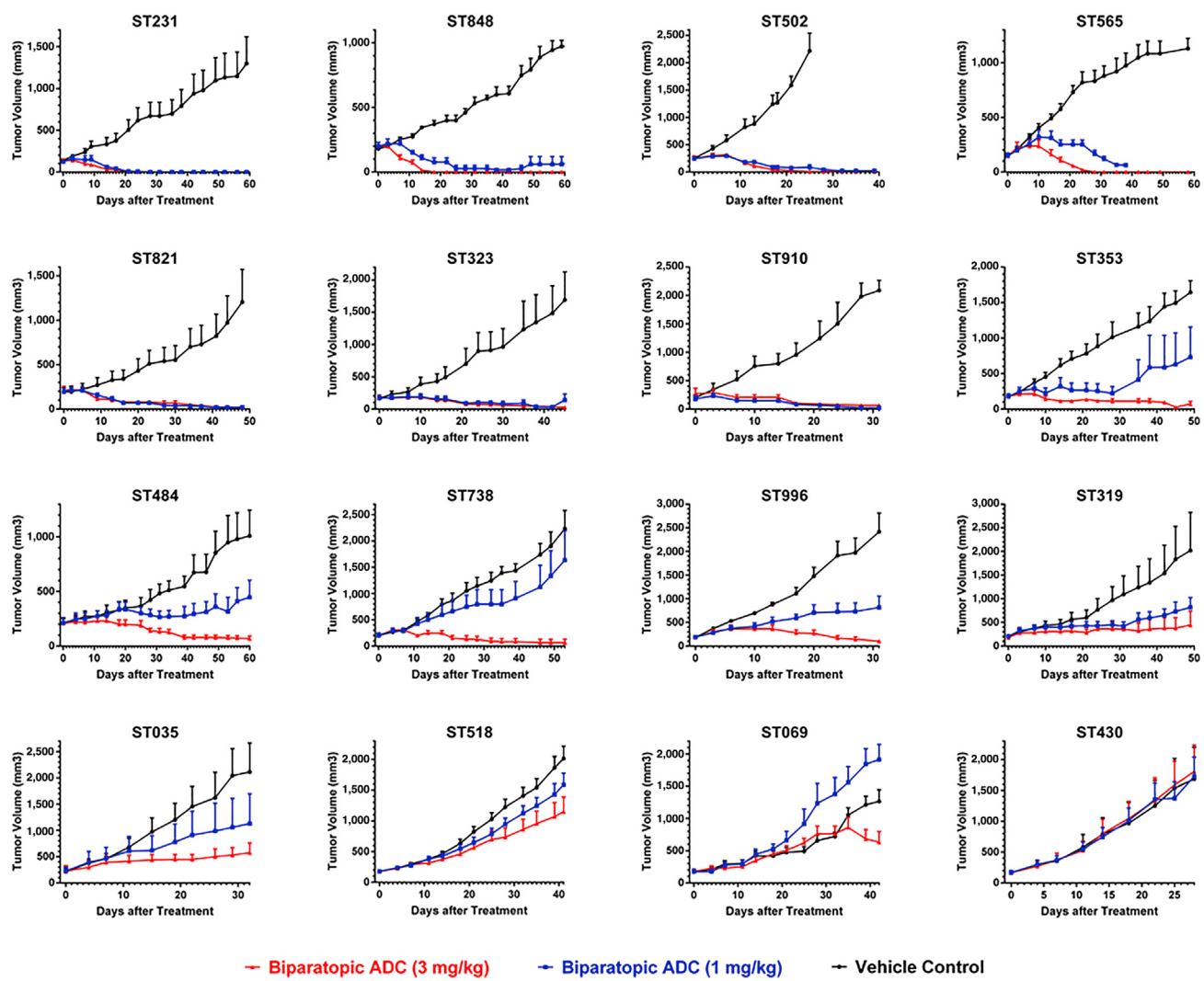


Figure 5. Biparatopic ADC Demonstrates Potent Anti-Tumor Activity in Primary Breast Cancer Models Representing HER2-Negative/T-DM1 Ineligible Patients

The specification of the primary tumor model is described in Table 2. Tumor-bearing mice were treated weekly with the biparatopic ADC at 1 or 3 mg/kg for a total of four doses. Tumor growth curves showing the mean tumor volume (mm^3) \pm SEM ($n = 5$).

expression system: the HER2-positive NCI-N87 cell line stably expressed the green fluorescent protein (GFP) and the HER2-null MDA-MB-468 cell line stably expressed the red fluorescent protein (RFP). Both cell lines were independently confirmed for in vitro sensitivity to the biparatopic ADC and T-DM1; and results showed that either the biparatopic ADC or T-DM1 was able to kill the NCI-N87/GFP cells but not the MDA-MB-468/RFP cells. We then mixed the two cell lines at an optimized ratio that was determined by their growth rates, and co-cultured the cells for 2 days. Cells were then treated with the biparatopic ADC, T-DM1, or control antibodies for 4 days and live cells were analyzed by flow cytometry. As shown in Figure 6, the biparatopic ADC, but not T-DM1 or isotype control ADC, was able to kill both HER2-positive cells and HER2-null cells that were in the co-culture. This demonstrates that the biparatopic ADC has bystander killing activity.

Biparatopic ADC Demonstrates an Acceptable Safety Profile in Cynomolgus Monkeys

The nonclinical safety of the biparatopic ADC was assessed in cynomolgus monkeys in a repeat-dose, intravenous, good-laboratory-practice (GLP) toxicology study. Cynomolgus monkey was selected as a relevant species for the toxicity study after the biparatopic ADC demonstrated significant cross-binding activity to human and cynomolgus monkey HER2 (Figure S1C), comparable binding affinity with the recombinant human and monkey HER2 proteins ($K_D = 137$ and 68.9 pM, respectively, determined by Biacore analysis), and ability to bind to the cynomolgus monkey fibrosis cell line Cynom K1 in flow cytometry (data not shown). In the repeat-dose GLP toxicology study needed for the regulatory submission of an investigational new drug, we paid specific attention to the target organs (e.g., cardiovascular systems, skin, and gastrointestinal tract) that are known to express a low level of HER2 receptor. The major adverse

Table 2. In Vivo Anti-Tumor Response to the Biparatopic ADC Treatment in a Panel of Primary Breast Cancer Models Representing HER2-Negative/T-DM1 Ineligible Patients

Breast Cancer PDX Models				Response ^a				
No.	Model	Cancer Subtype	HercepTest		HERmark (Mean ± SD) ^c	HER2Low Test (H-M-L) ^e	Response ^a	
			Intensity ^b	% Cells			1 mg/kg	3 mg/kg
1	ST231	TN, INFLAM	1+	40	18 ± 6	H	-100%*	-100%*
2	ST848	TN	0	-	9 ± 3	M	-70%*	-100%*
3	ST502	TN, INV-DC	2+	40	32 ± 2	H	-70%*	-97%*
4	ST565	ER+, INV-DC	2+	20	31 ± 7	H	-53%*	-100%*
5	ST821	TN	2+	35	20 ± 4	H	-90%*	-91%*
6	ST323	ER+, INV-DC	0	-	22 ± 2	H	-77%*	-82%*
7	ST910	TN, INV-CAR	1+	10	21 ± 7	H	-88%*	-75%*
8	ST455B	TN, CAR	1+	70	13 ± 3	H	12%†	-100%*
9	ST353	ER+, DC	1+	10	15 ± 4	H	34%‡	-85%*
10	ST484	ER+, INV-DC	1+	15	14 ^d	H	26%‡	-68%*
11	ST738	TN, INV	0	-	19 ± 1	H	67%‡	-67%*
12	ST996	TN, CAR	1+	10	19 ± 6	H	28%‡	-42%*
13	ST319	TN, BRCA ^{MUT}	2+	60	19 ± 1	H	32%‡	12%†
14	ST035	TN, INFLAM	0	-	14 ± 1	L	45%‡	17%†
15	ST518	TN, INV-LOB CAR	1+	10	10 ± 1	L	74%‡	53%‡
16	ST069	TN, INFLAM	0	-	21 ± 4	H	159%‡	42%‡
17	ST430	TN, INFILT-CAR	1+	10	22 ± 4	H	103%‡	108%‡

HER2 expression in tumors examined by three HER2-testing methods: HercepTest, HERmark, and HER2Low Test.

^aIn vivo anti-tumor response to the biparatopic ADC is determined by the tumor volume changes following the treatment. Tumor volume at the beginning of treatment is referred as the initial tumor volume (ITV); tumor volume at the time showing maximal response to the biparatopic ADC treatment is referred as the end tumor volume (ETV). If ETV is less than ITV, the anti-tumor response is calculated as follows: [(ETV – ITV)/ITV] × 100%. Otherwise the anti-tumor response is expressed as percent tumor volume change in the treatment arm relative to the vehicle control arm: [(ETV – ITV)_{treatment}/ (ETV – ITV)_{vehicle}] × 100%. Response to the treatment ranked as “regression” (marked with *) if it is less than -20%, “stasis” (marked with †) if it is in the range between -20% and 20%, and “progression” (marked with ‡) if it is more than 20%.

^bHercepTest is an approved, IHC-based, companion diagnosis for detecting HER2 protein overexpression in tumors. HER2 levels are categorized as 3+ (positive), 2+ (equivocal), 1+ and 0 (negative).

^cHERmark is an antibody-based, proximity-directed photochemical reaction assay for measuring the HER2 protein level in tumor tissues. The assay was conducted by Monogram Biosciences (San Francisco, CA) under a service agreement. The results are presented as means ± SD (n = 3).

^dn = 1.

^eThe HER2Low Test is an IHC assay developed by AstraZeneca and Dako to assess HER2 expression levels in HER2 non-overexpressing tumors. HER2 levels that are classified as HercepTest negative or equivocal (0, 1, and 2+) are categorized in this HER2Low Test as high (H), medium (M), and low (L).

effects observed following administration of the biparatopic ADC in monkeys were consistent with the mechanism of action of the tubulysin warhead and were largely related to the known safety profile of a microtubule-inhibiting agent that targets rapidly dividing cells (Poon et al., 2013; Sapra et al., 2013), as the unconjugated biparatopic antibody did not induce any adverse effects in monkeys at all doses that had been tested. The dose-limiting toxicity caused by the biparatopic ADC in monkeys is epithelial degeneration in the gastrointestinal tract. Despite a marginal level of HER2 expression on cardiomyocytes, there was no evidence of cardiotoxicity, as assessed by electrocardiogram, cardiac troponin I levels, and detailed histopathological evaluation in the GLP toxicity study. In addition, an in vitro electrophysiological assay with a cell line expressing human recombinant voltage-gated cardiac ion channel hERG indicated that the free tubulysin warhead AZ13599185 did not induce significant inhibition of hERG channel function at the projected therapeutic doses. Moreover, unlike T-DM1, which is well known to cause dose-limiting thrombocytopenia (Uppal et al., 2015), the bipara-

topic ADC did not cause dose-limiting adverse effects on platelets in monkeys. Overall, the safety profile and therapeutic index of the biparatopic ADC were adequate to transition into phase I clinical trials.

DISCUSSION

Sela and coworkers have reported that the combination of two anti-HER2 monoclonal antibodies that bind distinct epitopes can induce receptor downregulation (Friedman et al., 2005; Ben-Kasus et al., 2009). It is explained by their lattice model suggesting that a mixture of monoclonal antibodies may engage with the antigen at different epitopes to form large receptor-antibody lattices at the cell surface, which are ultimately endocytosed and sorted for lysosomal degradation. Pluckthun and coworkers have described a bispecific anti-EGFR designed ankyrin repeat proteins (DARPins) that are able to downregulate cell surface EGFR levels by inhibiting receptor recycling (Boersma et al., 2011). These prior works led us to hypothesize

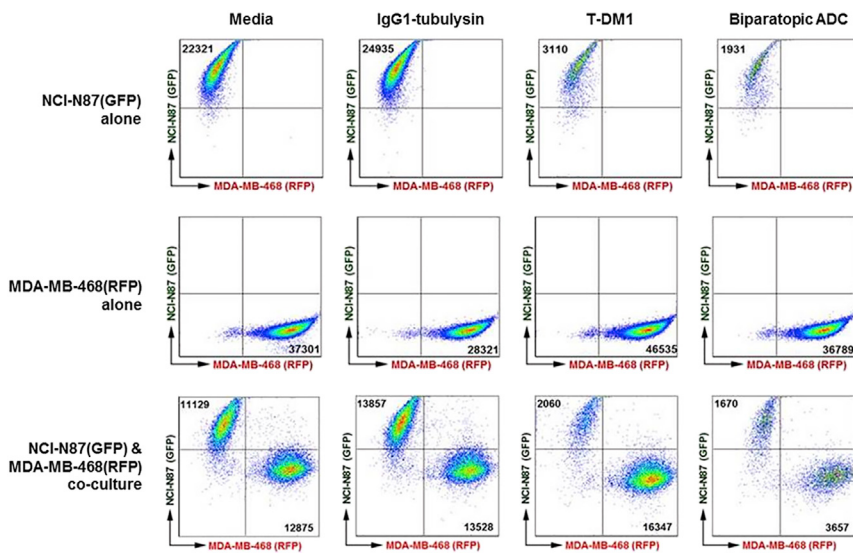


Figure 6. Biparatopic ADC Demonstrates Strong Bystander Killing Activity

NCI-N87/GFP cells and MDA-MB-468/RFP cells were cultured alone, or mixed at a ratio of 2.5:1 and co-cultured for 2 days, and then treated with 5 nM ADC for 4 days. Graphs show the representative images from flow cytometry analyses. Numbers shown in the upper-left and lower-right corners are the live cell numbers for NCI-N87/GFP and MDA-MB-468/RFP, respectively.

that a bivalent biparatopic antibody targeting two non-overlapping epitopes on HER2 would be effective in cross-linking receptors and thereby promoting the endocytosis and altering the receptor intracellular trafficking pathway from recycling to lysosomal degradation. In this study, we have generated several lines of evidence to support this hypothesis. First, the biparatopic antibody induces the formation of a large complex when incubated with HER2. Second, the biparatopic antibody elicits an enhanced internalization; over 90% of the cell surface HER2 is internalized within 60 min following the biparatopic antibody treatment in an HER2-overexpressing cell line. Third, the vast majority of internalized biparatopic antibody-HER2 complexes are co-localized with lysosomes as illustrated by confocal microscope imaging. Fourth, HER2 protein becomes undetectable by western blot analysis in cells incubated with the biparatopic antibody suggesting that the antibody-receptor complex is degraded after it is routed to lysosomes. In accordance with these data, the biparatopic ADC demonstrates superior in vitro and in vivo activities in killing cancer cells expressing either high or low levels of HER2. Overall, the biparatopic ADC in comparison with conventional ADCs such as T-DM1 is capable of delivering a greater quantity of cytotoxic agents into the cytoplasm of target cells due to its superior internalization, trafficking and ultimately degradation of the antibody-receptor complex in the lysosomes.

HER2 expression in normal tissues, although at a marginally detectable level when compared with tumors, has been observed in skin, cardiac muscle, epithelium of mammary gland, and the gastrointestinal tract (Press et al., 1990; Garratt et al., 2003; and M.C.R. and Y.J.L., unpublished tissue microarray data). Whether the biparatopic ADC would induce severe systemic toxicity due to its significantly enhanced activity in killing low HER2-expressing cells has been extensively investigated in this study. The key mechanism of action for the biparatopic ADC is to induce HER2 clustering, which triggers enhanced internalization and lysosomal trafficking and ultimately results in more toxins to be delivered into the target cells. The formation of the antibody-antigen matrix triggered by the biparatopic anti-

body is largely dependent on the HER2 level. As shown in Figure S2A, both the size and the quantity of complexes formed are decreased precipitately as the HER2 level drops, providing the biparatopic antibody concentration is fixed. The complex sizes are reduced to a range between 650 kDa and 1,300 kDa when the antibody/receptor ratio is 5; and the amount of complexes becomes nearly undetectable when the antibody/receptor ratio is more than 10. Accordingly, the extent of enhanced internalization induced by the biparatopic antibody becomes insignificant when the HER2 receptor density is below a certain level (Figure S2B). Also, the in vitro cytotoxic activity of the biparatopic ADC diminishes when the HER2 expression on cells is below a threshold level (Figure 3A and Table 1). These data suggest that the formation of a highly ordered, cross-linked meshwork complex requires the presence of a minimal number of HER2 receptors on the cell surface. The biparatopic ADC is unable to kill cells with a marginal (or below threshold) level of HER2. This is validated by both in vitro and in vivo studies showing that the biparatopic ADC has no or limited activity in T47D and MCF-7 cells in culture and it is inactive in the NCI-H69 model in mice. More importantly, the toxicity study in cynomolgus monkeys suggests that the biparatopic ADC has an acceptable safety profile that is in line with the expected toxicities for a microtubule inhibitor that targets rapidly dividing cells. In addition, the biparatopic ADC did not induce evident cardio-toxicity in monkeys, as it is a major adverse event associated with HER2-targeted therapies.

The biparatopic ADC has shown potent inhibitory activity in both in vitro tumor cells and an in vivo tumor model that have relapsed from T-DM1 treatment. Further investigation suggests that multiple mechanisms associated with the biparatopic ADC may contribute to its ability to overcome the acquired resistance. Quantitative flow cytometry analysis indicates that all four T-DM1 resistant cell lines have significantly reduced HER2 expression on the cell surface (60%–95% reduction) after the continuous treatment of T-DM1 (data not shown). This is consistent with previous reports from preclinical studies suggesting that downregulation of target expression is the primary mechanism of acquired resistance to T-DM1 (Burris et al., 2011; LoRusso et al., 2011). Owing to its ability to kill tumor cells expressing low levels of HER2, the biparatopic ADC is able to overcome T-DM1 resistance caused by downregulation of HER2 expression. In addition, we have observed that, in cell lines such as BT474 whose proliferation is addicted to the HER2-mediated

signaling pathways, upregulation of multi-drug resistance transporter/multi-drug resistance associated protein (MDR/MRP) efflux pumps appears to be another major mechanism of acquired resistance to T-DM1 (data not shown). Efflux pumps responsible for the DM1 resistance may not effectively transport tubulysin due to their structural difference and therefore do not result in cross-resistance to the tubulysin-based ADC. Furthermore, it is known that overexpression of heregulins can lead to resistance to trastuzumab as well as a number of chemotherapeutic agents used in the treatment of breast cancer (Tang et al., 1996; Hegde et al., 2013; Sergina et al., 2007; Garrett et al., 2011). Lewis Phillips et al. (2014) recently reported that the presence of heregulin-1 β attenuated the cytotoxic activity of T-DM1 in a subset of HER2-overexpressing cancer cell lines and co-treatment with pertuzumab reversed this inhibitory effect, suggesting that the heregulin-activated HER2-HER3 heterodimerization pathway might mediate the T-DM1 resistance. The biparatopic ADC contains the 39S Fv arm, which blocks the ligand-induced HER2-HER3 receptor dimerization. Thus, the dimerization-blocking ability inherent in the biparatopic ADC may also contribute to its activity against T-DM1-resistant cells where the increased level of heregulins in the tumor microenvironment is the cause of resistance.

In summary, we have developed a unique biparatopic HER2-targeting ADC that has multiple features enabling it to effectively kill tumor cells. These features include (1) efficient cytoplasmic delivery of cytotoxin by redirecting the HER2 intracellular trafficking from recycling to lysosomal degradation; (2) coupled with a different microtubule inhibitor that may bypass the DM1 efflux pumps; (3) synergistic inhibition of both ligand-independent and ligand-dependent mitogenic signaling pathways that may drive tumor growth and drug resistance; and (4) a bystander effect that kills heterogeneous cancer cell populations. The ability of the biparatopic ADC to kill both T-DM1 resistant and low HER2-expressing tumor cells represents a unique opportunity to provide benefit to patients with a high unmet medical need and warrants investigation in the clinic.

EXPERIMENTAL PROCEDURES

Cell Culture, Reagents and Biparatopic ADC Generation

Cell lines JIMT-1 and RT-112 were obtained from Leibniz Institute DSMZ. The MCF7-GTU cell line was provided by Dr. Robert Clarke at Georgetown University under a material license agreement. All other cell lines were obtained from American Type Culture Collection. The lentiviral vectors pLKO.1-puro-CMV-TurboGFP and pLKO.1-puro-CMV-TagRFP used to generate the NCI-N87/GFP and MDA-MB-468/RFP cell lines were purchased from Sigma-Aldrich. Herceptin (trastuzumab) and Perjeta (pertuzumab) were purchased from Hoffmann-La Roche. Biparatopic antibody construction was carried out as described (Dimasi et al., 2009). Tubulysin variant AZ13599185 was conjugated to antibody via the maleimidocaproyl linker through the maleimide-thiol reaction. Briefly, after reduction and oxidation, the biparatopic antibody was site-specifically conjugated with the maleimidocaproyl-functionalized tubulysin AZ13599185. The biparatopic ADC was purified using type II ceramic hydroxyapatite chromatography to remove macromolecular aggregates and free drug. Conjugation efficiency and the drug/antibody ratio were determined using UV- and mass spectrometry-based methods following standard procedures.

In Vitro Cell Proliferation Assay

Cells were seeded in 96-well plates and treated with antibody or ADC in a step-wise 1:4 serial dilution series for 3–6 days, depending on the growth kinetics of each cell line. Cell viability was determined using Cell Titer Glo from Promega

according to the manufacturer's instructions. Data were analyzed with GraphPad Prism software and are presented as percent growth inhibition relative to the untreated control.

Immunoprecipitation and Western Blot Analysis

Cells were pre-incubated with 5 nM antibody to be tested for 20 min and then stimulated with 1 nM heregulin-1 β for 10 min. To detect HER2:HER3 receptor dimerization, the cell lysates were incubated with a mouse anti-HER2 antibody (clone 44 E7, Cell Signaling) and the immunocomplex was precipitated using the Classic IP Kit from Thermo Scientific according to the manufacturer's instructions. HER2 and HER3 proteins in the immunoprecipitated samples were examined by western blot with a rabbit anti-HER2 monoclonal antibody (clone 29D8, Cell Signaling) and a rabbit polyclonal antibody against HER3 (C-17, Santa Cruz Biotechnology), respectively.

Internalization Assay

Cells were incubated with antibody or an antibody combination (50 nM each antibody) on ice for 1 hr and then washed to remove unbound antibodies. An aliquot of cells remained on ice and the rest were incubated at 37°C for different periods of time. Cells were fixed in 2% paraformaldehyde for 20 min and then stained with Alexa-Fluor 488-labeled antibody against human IgG and analyzed by flow cytometry and FlowJo software. Receptor-antibody complex internalization was calculated as percent mean fluorescent intensity (MFI) loss at 37°C relative to that on ice after subtracting the background value of MFI derived from the untreated control.

Confocal Microscopy

To illustrate receptor-antibody internalization and lysosomal trafficking, cells were incubated with 50 nM antibody to be tested at 37°C for different periods of time, and then washed, fixed, and permeabilized using fixation/permeabilization solution (BD Biosciences) according to the manufacturer's instructions. Cells were stained with Alexa-Fluor 488-labeled antibody against human IgG to visualize receptor-antibody complex (green), and mouse anti-human LAMP-1 (clone H4A3, BD Biosciences) followed by Alexa-Fluor 647-labeled anti-mouse IgG to visualize the lysosomes (red). To examine the intracellular microtubule network, cells were treated with 5 nM ADC to be tested at 37°C overnight. Cells were fixed in 2% paraformaldehyde for 20 min and then permeabilized using Triton X-100. Cells were stained with Alexa-Fluor 488-labeled rabbit antibody against human α -tubulin (clone 11H10, Cell Signaling). After staining, cells were coverslipped with ProLong Gold Antifade Reagent containing DAPI (Invitrogen) and analyzed by a Leica SP5 confocal microscope and the Leica Application Suite Advanced Fluorescence software suite.

Quantitative Flow Cytometry

HER2 receptor density on cells was determined by Quantum 647 MESF (Bang Laboratories) following the manufacturer's recommended protocol. Briefly, cells (3×10^5) were resuspended in 96-well plates and stained with Alexa-Fluor 647-labeled 39S antibody on ice at a pre-determined saturating concentration for each cell line. After staining, cells were fixed in 2% paraformaldehyde and analyzed by flow cytometry and FlowJo software along with Bang Laboratories' standard beads. Relative receptor density was calculated based on MFI values and the standard curve generated from Bang Laboratories' standard beads.

Tumor Xenograft Studies

All mouse experiments were carried out in compliance with the guidelines published by the Association for Assessment and Accreditation of Laboratory Animal Care (AAALAC) and protocols approved by the MedImmune Institutional Animal Care and Use Committee. Tumor cells or tumor tissue fragments were implanted subcutaneously or orthotopically in athymic nude mice between 4 and 8 weeks of age. When tumors reached the appropriate tumor volume range (typically 150–250 mm³), animals were randomized into treatment and control groups and dosing was initiated. Tumor-bearing mice were dosed once weekly for a total of four doses with test articles via intravenous injection unless otherwise specified. Animals were observed daily and tumor dimensions and body weight were measured and recorded twice weekly. Tumor volumes were calculated using the following formula: tumor volume = $\pi \div 6(\text{length} \times \text{width}^2)$.

Statistical Analyses

Quantitative data were analyzed by one-way ANOVA or Student's *t* test. Difference with $p < 0.05$ was considered statistically significant. Combination treatment was analyzed for synergism using a Bliss independence-based two-stage response surface model as described (Zhao et al., 2014). Combination with interaction index (I) > 0 was considered synergistic.

SUPPLEMENTAL INFORMATION

Supplemental Information includes four figures and can be found with this article online at <http://dx.doi.org/10.1016/j.ccr.2015.12.008>.

AUTHOR CONTRIBUTIONS

J.Y.L. conceived and designed the study, analyzed data, supervised the overall study, and wrote the manuscript. S.R.P. performed most of the experiments. V.M.M. carried out the internalization experiment. L.K.W. conducted some *in vivo* experiments. M.C.R. oversaw the histologic study and performed the histopathologic analysis. M.J.M.H. conducted the toxicology studies and safety assessment. C.G., N.D., B.Z.B., R.L.F., A.Q.Y., L.X., and J.L. contributed to the antibody design and construction. B.Z.B. and R.L.F. also performed the antibody-drug conjugation. H.F. conducted the SEC-MALS assay. D.T. contributed to the design of tubulysin variant AZ13599185. X.W., H.W., R.D., J.K.O., and S.R.C. contributed to the study design and data analysis. All authors participated in revising the manuscript.

ACKNOWLEDGMENTS

We thank D. Jenkins (MedImmune) for helpful comments on the manuscript. We thank L. Clarke, S. Wilson, and additional members of the Protein Sciences group (MedImmune) for providing various recombinant protein reagents and cell lines expressing GFP or RFP. We thank W. Zhao at the Biostatistics group (MedImmune) for helping with the statistical analysis for synergism. We also thank South Texas Accelerated Research Therapeutics (START) for conducting *in vivo* experiments in patient-derived xenograft (PDX) models under service agreements. START is an AAALAC accredited institution. The authors of this publication are employees of MedImmune LLC, or were employees of MedImmune LLC while they were involved in this work. This work was supported by MedImmune LLC.

Received: March 31, 2015

Revised: September 18, 2015

Accepted: December 15, 2015

Published: January 11, 2016

REFERENCES

- Austin, C.D., De Mazière, A.M., Pisacane, P.I., van Dijk, S.M., Eigenbrot, C., Sliwkowski, M.X., Klumperman, J., and Scheller, R.H. (2004). Endocytosis and sorting of ErbB2 and the site of action of cancer therapeutics trastuzumab and geldanamycin. *Mol. Biol. Cell* 15, 5268–5282.
- Ben-Kasus, T., Schechter, B., Lavi, S., Yarden, Y., and Sela, M. (2009). Persistent elimination of ErbB-2/HER2-overexpressing tumors using combinations of monoclonal antibodies: relevance of receptor endocytosis. *Proc. Natl. Acad. Sci. USA* 106, 3294–3299.
- Boersma, Y.L., Chao, G., Steiner, D., Wittrup, K.D., and Pluckthun, A. (2011). Bispecific designed ankyrin repeat proteins (DARPins) targeting epidermal growth factor receptor inhibit A431 cell proliferation and receptor recycling. *J. Biol. Chem.* 286, 41273–41285.
- Burris, H.A., Rugo, H.S., Vukelja, S.J., Vogel, C.L., Borson, R.A., Limentani, S., Tan-Chiu, E., Krop, I.E., Michaelson, R.A., Girish, S., et al. (2011). Phase II study of the antibody drug conjugate trastuzumab-DM1 for the treatment of human epidermal growth factor receptor 2 (HER2)-positive breast cancer after prior HER2-directed therapy. *J. Clin. Oncol.* 29, 398–405.
- Cartilage, S., Dong, J., Foltz, I., Hickinson, M., and Kang, S.J. (June 2010). Human Antibodies to ErbB2, US Patent Application Publication No. 20100158926A1.
- Dimasi, N., Gao, C., Fleming, R., Woods, R.M., Yao, X.T., Shirinian, L., Kiener, P.A., and Wu, H. (2009). The design and characterization of oligospecific antibodies for simultaneous targeting of multiple disease mediators. *J. Mol. Biol.* 393, 672–692.
- Friedman, L.M., Rinon, A., Schechter, B., Lyass, L., Lavi, S., Bacus, S.S., Sela, M., and Yarden, Y. (2005). Synergistic down-regulation of receptor tyrosine kinases by combinations of mAbs: implications for cancer immunotherapy. *Proc. Natl. Acad. Sci. USA* 102, 1915–1920.
- Garratt, A.N., Ozcelik, C., and Birchmeier, C. (2003). ErbB2 pathways in heart and neural diseases. *Trends Cardiovasc. Med.* 13, 80–86.
- Garrett, J.T., Olivares, M.G., Rinehart, C., Granja-Ingram, N.D., Sánchez, V., Chakrabarty, A., Dave, B., Cook, R.S., Pao, W., McKinley, E., et al. (2011). Transcriptional and posttranslational up-regulation of HER3 (ErbB3) compensates for inhibition of the HER2 tyrosine kinase. *Proc. Natl. Acad. Sci. USA* 108, 5021–5026.
- Hegde, G.V., de la Cruz, C.C., Chiu, C., Alag, N., Schaefer, G., Crocker, L., Ross, S., Goldenberg, D., Merchant, M., Tien, J., et al. (2013). Blocking NRG1 and other ligand-mediated Her4 signaling enhances the magnitude and duration of the chemotherapeutic response of non-small cell lung cancer. *Sci. Transl. Med.* 5, 171ra18.
- Huang, W., Reinholtz, M., Weidler, J., Yolanda, L., Paquet, A., Whitcomb, J., Lingle, W., Jenkins, R.B., Chen, B., Larson, J.S., et al. (2010). Comparison of central HER2 testing with quantitative total HER2 expression and HER2 homodimer measurements using a novel proximity-based assay. *Am. J. Clin. Pathol.* 134, 303–311.
- Junttila, T.T., Akita, R.W., Parsons, K., Fields, C., Lewis Phillips, G.D., Friedman, L.S., Sampath, D., and Sliwkowski, M.X. (2009). Ligand-independent HER2/HER3/PI3K complex is disrupted by trastuzumab and is effectively inhibited by the PI3K inhibitor GDC-0941. *Cancer Cell* 15, 429–440.
- Kovtun, Y.V., and Goldmacher, V.S. (2007). Cell killing by antibody-drug conjugates. *Cancer Lett.* 255, 232–240.
- Kurata, T., Tsurutani, J., Fujisaka, Y., Okamoto, W., Hayashi, H., Kawakami, H., Shin, E., Hayashi, N., and Nakagawa, K. (2014). Inhibition of EGFR, HER2 and HER3 signaling with AZD8931 alone and in combination with paclitaxel: phase I study in Japanese patients with advanced solid malignancies and advanced breast cancer. *Invest. New Drugs* 32, 946–954.
- Lambert, J.M., and Chari, R.V. (2014). Ado-trastuzumab Emtansine (T-DM1): an antibody-drug conjugate (ADC) for HER2-positive breast cancer. *J. Med. Chem.* 57, 6949–6964.
- Lewis Phillips, G.D., Li, G., Dugger, D.L., Crocker, L.M., Parsons, K.L., Mai, E., Blättler, W.A., Lambert, J.M., Chari, R.V., Lutz, R.J., et al. (2008). Targeting HER2-positive breast cancer with trastuzumab-DM1, an antibody-cytotoxic drug conjugate. *Cancer Res.* 68, 9280–9290.
- Lewis Phillips, G.D., Fields, C.T., Li, G., Dowbenko, D., Schaefer, G., Miller, K., Andre, F., Burris, H.A., III, Albain, K.S., Harbeck, N., et al. (2014). Dual targeting of HER2-positive cancer with trastuzumab emtansine and pertuzumab: critical role for neuregulin blockade in antitumor response to combination therapy. *Clin. Cancer Res.* 20, 456–468.
- Llombart-Cussac, A., Pivot, X., Biganzoli, L., Cortes-Funes, H., Pritchard, K.I., Pierga, J.Y., Smith, I., Thomassen, C., Srock, S., Sampayo, M., et al. (2014). A prognostic factor index for overall survival in patients receiving first-line chemotherapy for HER2-negative advanced breast cancer: an analysis of the ATHENA trial. *Breast* 23, 656–662.
- LoRusso, P.M., Weiss, D., Guardino, E., Girish, S., and Sliwkowski, M.X. (2011). Trastuzumab emtansine: a unique antibody-drug conjugate in development for human epidermal growth factor receptor 2-positive cancer. *Clin. Cancer Res.* 17, 6437–6447.
- Nordstrom, J.L., Gorlatov, S., Zhang, W., Yang, Y., Huang, L., Burke, S., Li, H., Ciccarone, V., Zhang, T., Stavenhagen, J., et al. (2011). Anti-tumor activity and toxicokinetics analysis of MGAH22, an anti-HER2 monoclonal antibody with enhanced Fc γ receptor binding properties. *Breast Cancer Res.* 13, R123.
- Pedersen, H.C., Thomsen, A., Jensen, K., Jakobsen, K., Wellings, B., Dalglish, G., Tosh, K., Harbron, C., and Walker, J. (2013). A new, highly sensitive IHC test for the detection of HER2 protein in breast cancer (BC) tissue. *Cancer Res.* 73, 2384.

- Poon, K.A., Flagella, K., Beyer, J., Tibbitts, J., Kaur, S., Saad, O., Yi, J.H., Girish, S., Dybdal, N., and Reynolds, T. (2013). Preclinical safety profile of trastuzumab emtansine (T-DM1): mechanism of action of its cytotoxic component retained with improved tolerability. *Toxicol. Appl. Pharmacol.* 273, 298–313.
- Press, M.F., Cordon-Cardo, C., and Slamon, D.J. (1990). Expression of the HER-2/neu proto-oncogene in normal human adult and fetal tissues. *Oncogene* 5, 953–962.
- Roepstorff, K., Grovdal, L., Grandal, M., Lerdrup, M., and van Deurs, B. (2008). Endocytic downregulation of ErbB receptors: mechanisms and relevance in cancer. *Histochem. Cell Biol.* 129, 563–578.
- Roskoski, R.J. (2014). The ErbB/HER family of protein-tyrosine kinases and cancer. *Pharmacol. Res.* 79, 34–74.
- Sapra, P., Damelin, M., Dijoseph, J., Marquette, K., Geles, K.G., Golas, J., Dougher, M., Narayanan, B., Giannakou, A., Khandke, K., et al. (2013). Long-term tumor regression induced by an antibody-drug conjugate that targets 5T4, an oncofetal antigen expressed on tumor-initiating cells. *Mol. Cancer Ther.* 12, 38–47.
- Sergina, N.V., Rausch, M., Wang, D., Blair, J., Hann, B., Shokat, K.M., and Moasser, M.M. (2007). Escape from HER-family tyrosine kinase inhibitor therapy by the kinase-inactive HER3. *Nature* 445, 437–441.
- Sievers, E.L., and Senter, P.D. (2013). Antibody-drug conjugates in cancer therapy. *Annu. Rev. Med.* 64, 15–29.
- Slamon, D.J., Clark, G.M., Wong, S.G., Levin, W.J., Ullrich, A., and McGuire, W.L. (1987). Human breast cancer: correlation of relapse and survival with amplification of the HER-2/neu oncogene. *Science* 235, 177–182.
- Sorkin, A., and Goh, L.K. (2008). Endocytosis and intracellular trafficking of ErbBs. *Exp. Cell Res.* 314, 3093–3106.
- Spangler, J.B., Neil, J.R., Abramovitch, S., Yarden, Y., White, F.M., Lauffenburger, D.A., and Wittrup, K.D. (2010). Combination antibody treatment down-regulates epidermal growth factor receptor by inhibiting endosomal recycling. *Proc. Natl. Acad. Sci. USA* 107, 13252–13257.
- Spangler, J.B., Manzari, M.T., Rosalia, E.K., Chen, T.F., and Wittrup, K.D. (2012). Triepitopic antibody fusions inhibit cetuximab-resistant BRAF and KRAS mutant tumors via EGFR signal repression. *J. Mol. Biol.* 422, 532–544.
- Tagliabue, E., Balsari, A., Campiglio, M., and Pupa, S.M. (2010). HER2 as a target for breast cancer therapy. *Expert Opin. Biol. Ther.* 10, 711–724.
- Tang, C.K., Perez, C., Grunt, T., Waibel, C., Cho, C., and Lupu, R. (1996). Involvement of heregulin-beta2 in the acquisition of the hormone-independent phenotype of breast cancer cells. *Cancer Res.* 56, 3350–3358.
- Uppal, H., Doudement, E., Mahapatra, K., Darbonne, W.C., Bumbaca, D., Shen, B.Q., Du, X., Saad, O., Bowles, K., Olsen, S., et al. (2015). Potential mechanisms for thrombocytopenia development with trastuzumab emtansine (T-DM1). *Clin. Cancer Res.* 21, 123–133.
- Verma, S., Miles, D., Gianni, L., Krop, I.E., Welslau, M., Baselga, J., Pegram, M., Oh, D.Y., Diéras, V., Guardino, E., et al. (2012). Trastuzumab emtansine for HER2-positive advanced breast cancer. *N. Engl. J. Med.* 367, 1783–1791.
- Wiley, H.S. (2003). Trafficking of the ErbB receptors and its influence on signaling. *Exp. Cell Res.* 284, 78–88.
- Yarden, Y., and Sliwkowski, M.X. (2001). Untangling the ErbB signaling network. *Nat. Rev. Mol. Cell Biol.* 2, 127–137.
- Zhao, W., Sachsenmeier, K., Zhang, L., Sult, E., Hollingsworth, R.E., and Yang, H. (2014). A new Bliss independence model to analyze drug combination data. *J. Biomol. Screen* 19, 817–821.

Update

Cancer Cell

Volume 35, Issue 6, 10 June 2019, Page 948–949

DOI: <https://doi.org/10.1016/j.ccell.2019.05.010>

A Biparatopic HER2-Targeting Antibody-Drug Conjugate Induces Tumor Regression in Primary Models Refractory to or Ineligible for HER2-Targeted Therapy

John Y. Li,* Samuel R. Perry, Vanessa Muniz-Medina, Xinzhang Wang, Leslie K. Wetzel, Marlon C. Rebelatto, Mary Jane Masson Hinrichs, Binyam Z. Bezabeh, Ryan L. Fleming, Nazzareno Dimasi, Hui Feng, Dorin Toader, Andy Q. Yuan, Lan Xu, Jia Lin, Changshou Gao, Herren Wu, Rakesh Dixit, Jane K. Osbourn, and Steven R. Coats

*Correspondence: john.li@salubrisbio.com

<https://doi.org/10.1016/j.ccr.2019.05.010>

(Cancer Cell 29, 117–129; January 11, 2016)

In the originally published version of this article, in Figure 2E the representative immunoblots of lysates from antibody-treated cells did not indicate spliced lines between lane 7 and lane 8. When preparing the figure for publication, these lanes had been spliced together from the same immunoblot, as indicated in the corrected Figure 2E shown here, to remove an irrelevant lane. The authors apologize for any confusion this may have caused.



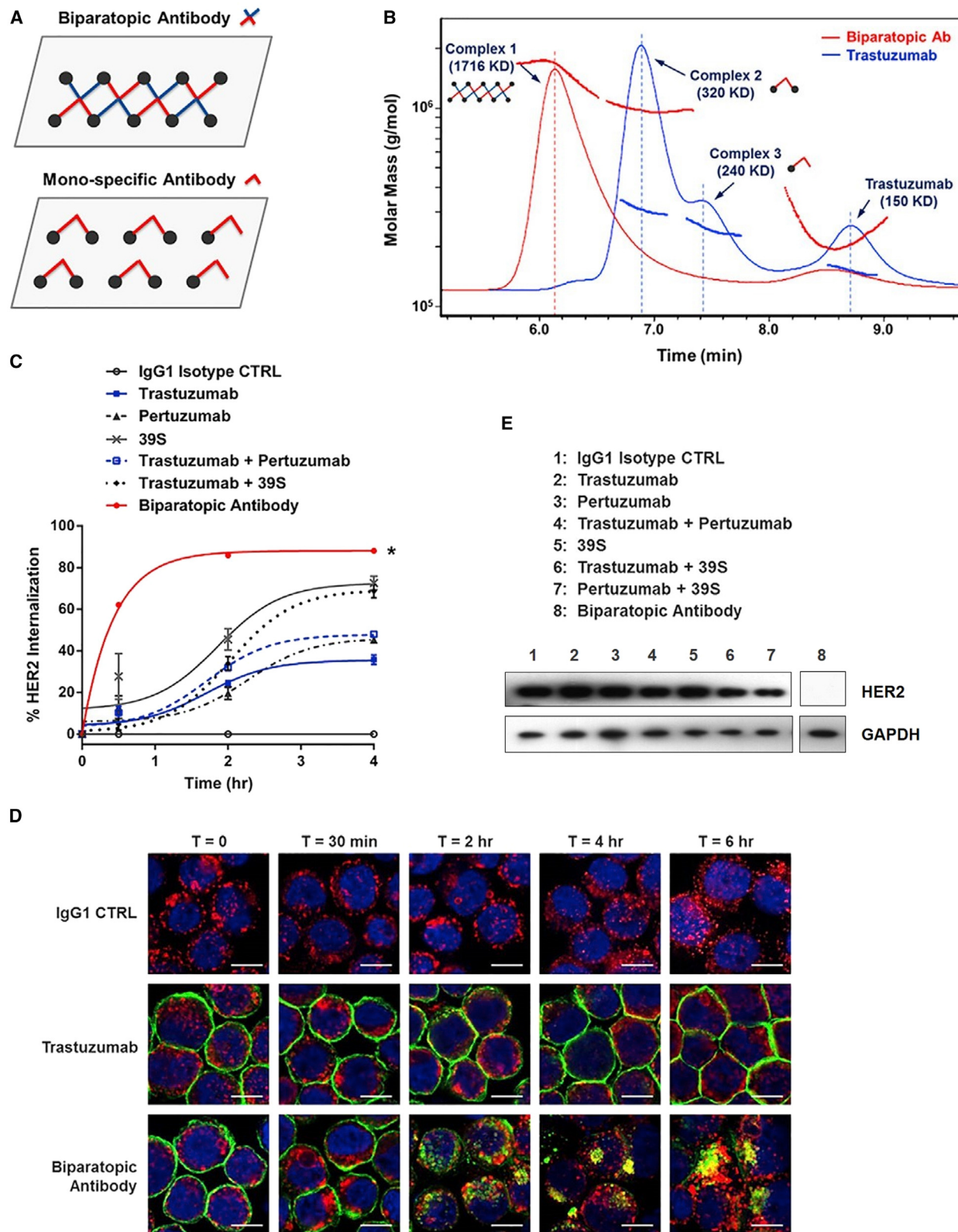


Figure 2. The Biparatopic Antibody Promotes HER2 Clustering and Lysosomal Degradation